

Novel Method for *In-Situ* Monitoring of Thickness of Silicon Wafer during Wet Etching

Chi-Yuan Lee*, Pei-Zen Chang¹, Yung-Yu Chen¹,
Ching-Liang Dai², Xuan-Yu Wang¹, Ping-Hei Chen³ and Shuo-Jen Lee

Department of Mechanical Engineering, Fuel Cell Research Center, Yuan Ze University,
135 Yuan-Tung Road, Chungli, 320
Taoyuan, Taiwan, R. O. C.

¹Institute of Applied Mechanics, National Taiwan University, No. 1, Sec. 4, Roosevelt Road,
106 Taipei, Taiwan, R. O. C.

²Department of Mechanical Engineering, National Chung Hsing University, 250 Kuo Kuang Road,
Taichung 402, Taiwan, R. O. C.

³Department of Mechanical Engineering, National Taiwan University, No. 1, Sec. 4,
Roosevelt Road, 106 Taipei, Taiwan, R. O. C.

(Received April 11, 2005; accepted September 26, 2005)

Key words: *in-situ* monitoring, plate wave sensor, Li-doped ZnO, IDT

In this investigation, we developed a plate wave sensor made on a Li-doped ZnO piezoelectric film for monitoring the thickness of a silicon membrane in real-time during wet etching. A novel method, which differs from any presented in previous work on etch-stop techniques, is developed to monitor *in-situ* the thickness of a silicon membrane during wet etching. In this work, in which the design wavelength of the interdigital transducers (IDT) is 40 μm , the method presented for measuring the thickness of a silicon membrane from 20 μm to 40 μm in real-time is highly accurate and simple to implement. Base on the same methodology, the proposed plate wave sensor also allows the thickness of a silicon membrane to be monitored from a few μm to hundreds of μm *in-situ*, depending on the periodicity of the IDT. The principles of the method, the detailed fabrication flow, the set-up for monitoring the thickness and the simulation and experimental results are all addressed. The theoretical and measured values differ by an error of less than 1.50 μm and are very close to each other.

1. Introduction

This investigation presents a novel method based on a plate wave sensor for monitoring *in-situ* the thickness of a silicon membrane during wet etching. Similar to accelerometers, pressure sensors, micro-flow sensors and micropumps, numerous micro-electro-mechanical system (MEMS) devices require that the silicon membrane thickness be known exactly. Precisely controlling the thickness of a silicon membrane during wet etching is important, because the thickness strongly influences post-processing and device performance. A

*Corresponding author, e-mail address: cylee@saturn.yzu.edu.tw

novel in-situ method, which differs from any in previous investigations of etch-stop techniques,⁽¹⁻⁴⁾ is developed to monitor the thickness of a silicon membrane during wet etching. An optical method for the in-situ monitoring of the thickness of the silicon diaphragm has been presented and its success in MEMS applications has been demonstrated.⁽¹⁾ However, that method can be applied to measure the thickness of a silicon membrane only between 2 and 20 μm , and the monitoring equipment is complex. The electrochemical and boron etch-stop methods can adequately control the thickness of a silicon membrane.^(2,3) The former involves difficulties in the batch process of wet etching; the latter may cause contamination and residual stress due to a heavily doped region. The authors have designed differently constructed sensors using the spectral analysis of surface waves (SASW) method, not a real-time method and a measurement tool to evaluate the thickness of the silicon membrane.⁽⁵⁾ However, the authors have also published reports in which the design wavelength of the IDT was 80 μm : the attenuation is large when the thickness of the silicon membrane is under 50 μm , so no experimental data concerning this area can be obtained. This method can be used to measure the thickness of a silicon membrane in real time from 50 μm to 80 μm .⁽⁶⁾ In this new work, in which the design wavelength of the IDT is changed to 40 μm , the method presented can measure the thickness of a silicon membrane in real time from 20 μm to 40 μm . Accordingly, the proposed plate wave sensor allows the thickness of a silicon membrane to be monitored from a few μm to hundreds of μm depending on the periodicity of the IDT. The principles of the method, the detailed fabrication flow, the set-up for measuring thickness and the simulation and experimental findings are all discussed.

2. Methodology

2.1 *Plate waves that propagate in a piezoelectric film based on a multilayer structure loaded with viscous liquid*

In this section, we consider the propagation of a plate wave in an anisotropic multilayer structure filled with viscous liquid. The result of the simulation shows the dispersion curve for phase velocity (frequency) with respect to the silicon thickness and compares it with the experimental result.

The eight-dimensional matrix formalism has been derived and applied to the propagation of plate waves in a piezoelectric film based on a multilayered structure and filled with viscous liquid.^(7,8) This formulation derives the dispersion equation of plate waves in such a structure from continuity conditions at the solid-liquid interface. The size of the matrix in the computation is independent of the number of layers. This characteristic is helpful in analyzing the behavior of waves in a multilayered structure.

Consider a piezoelectric film based on a silicon substrate filled with viscous liquid in the half-space, where the interface is at $z = H$, as shown in Fig. 1. According to the eight-dimensional matrix formalism, at the interface, the relationship between the generalized traction vector T and the generalized velocity vector V is expressed as⁽⁹⁾

$$T(H^-) = GV(H^-), \quad (1)$$

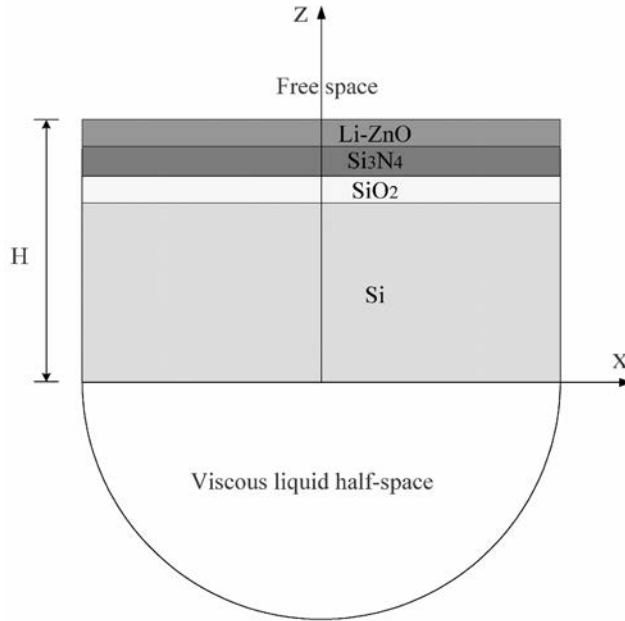


Fig. 1. Configuration of piezoelectric film based on silicon substrate filled with viscous liquid in half-space.

where G is the impedance tensor and H is the thickness of a multilayered structure. In the viscous liquid half-space, since only up-going waves exist, the global impedance is equivalent to the up-going wave impedance Z_1 . Consequently, the corresponding relationship at the boundary of the viscous liquid is given by

$$T_1(H^+) = Z_1 V_1(H^+). \quad (2)$$

At the liquid-solid interface, the stress, the particle velocity, the electric potential and the electric displacement must satisfy the continuity condition:

$$T(H^-) = T_1(H^+), V(H^-) = V_1(H^+) = V(H). \quad (3)$$

From eqs. (1)–(3), we obtain

$$(G - Z_1)V(H) = 0. \quad (4)$$

The nontrivial solution of the generalized velocity vector $V(H)$ exists only if

$$\det(G - Z_1) = 0. \quad (5)$$

Equation (5) is also called the dispersion equation for the propagation of plate waves in a piezoelectric film based on a silicon substrate with a half-space filled with viscous liquid.

Based on the foregoing formulation, the dispersion characteristics of the viscous liquid-filled Si (308.40 μm) / SiO₂(1000 Å) / Si₃N₄(1500 Å) / Li-ZnO(1.56 μm) multilayered system are studied. The epitaxial relationships are that the c-axis of Li-ZnO is parallel to the surface of the (100) silicon substrate, and the Rayleigh wave propagates along the X-axis of the Li-ZnO film and in the <100> direction of the silicon substrate. The relevant constants used in the calculations are adopted from ref. (10). Table 1 lists the material constants used in this calculation. Figure 2 presents the results of a simulation of phase velocity with respect to silicon thickness. According to the simulation, the phase velocity approaches the velocity of the Rayleigh wave of silicon as the thickness of silicon increases. When the thickness of the silicon is less than the wavelength of an acoustic wave, the surface acoustic wave and the bulk wave combine into a plate wave, whose phase velocity varies with the thickness of the silicon substrate. The simulation indicates that the attenuation increases as the thickness of the silicon membrane decreases, as shown in Fig. 3. The attenuation of the plate wave has minimal effect on the determination of silicon membrane thickness if the membrane thickness is greater than 35 μm . The cause of the

Table 1
Material constants used in simulation.

		ZnO	Silicon	Water
Elastic constants (10 ¹¹ N/m ²)	C_{11}	2.10	1.657	
	C_{12}	1.205	0.639	
	C_{13}	1.05		
	C_{33}	2.11		
	C_{44}	0.423	0.796	
Piezoelectric constants (C/m ²)	e_{15}	-0.48		
	e_{31}	-0.573		
	e_{33}	1.321		
Relative dielectric constants	ϵ_{11}	8.55	11.7	80.359
	ϵ_{33}	10.2		
Mass density (10 ³ kg/m ³)	ρ	5.67	2.332	0.997
Longitudinal wave velocity (m/s)	C_L			1500
Viscosity (10 ⁻⁴ Ns/m ²)	μ_L			8.9

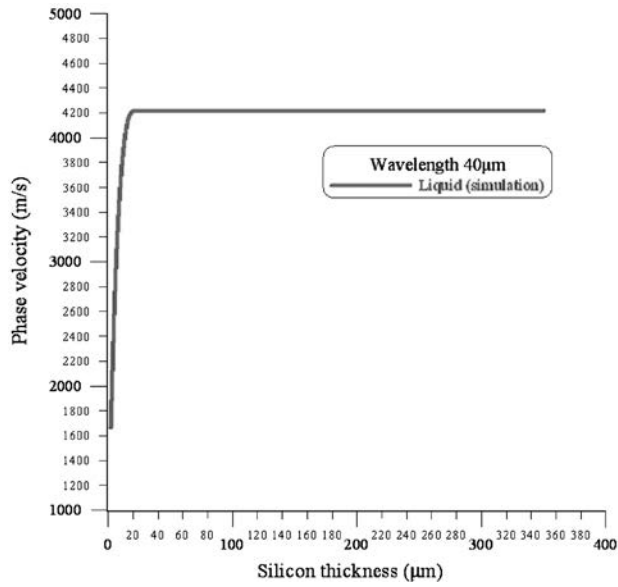


Fig. 2. Dispersion curve of viscous liquid-filled silicon substrate.

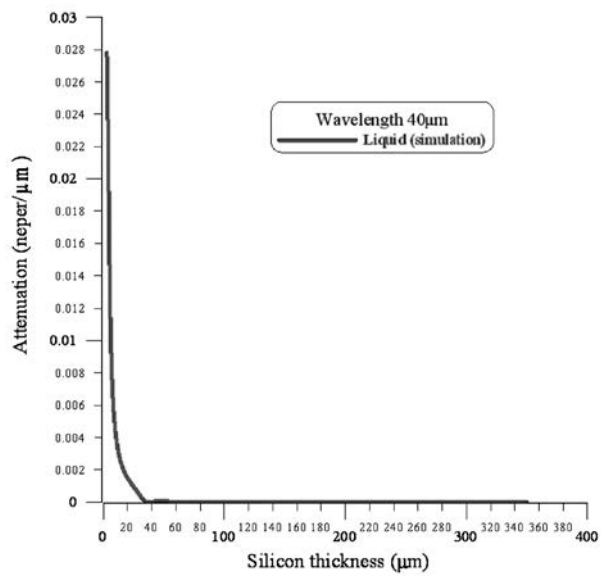


Fig. 3. Attenuation of plate wave of viscous-liquid-filled silicon substrate.

attenuation is primarily the energy leakage into the liquid half-space. The attenuation increases as the thickness of silicon membrane decreases. In this design, in which the wavelength of the IDT is 40 μm , the attenuation becomes large when the thickness of the silicon membrane is less than 20 μm , so no experimental data concerning this area can be obtained.

2.2 Design of plate wave sensor

A plate wave sensor, as shown in Fig. 4, is fabricated on a double polished (100) silicon substrate. The plate wave sensor (Fig. 4) contains two ports of split-electrode IDTs mounted on a piezoelectric film. The IDT that carries out electroacoustic coupling can translate acoustic energy into electrical energy on the piezoelectric film.⁽¹¹⁾ The material of the piezoelectric film is Li-ZnO, which is made from ZnO film with Li doping. The Li-ZnO film exceeds the ZnO film in resistivity.⁽¹²⁾ The Li-ZnO film is deposited by sputtering technology. Figure 5 presents X-ray diffraction (XRD) scans of a Li-ZnO film, which indicate that a Li-ZnO film exhibits a strong c-axis orientation. Figure 6 presents the scanning electron microscope (SEM) micrographs of the optimized 1.56 μm thick Li-ZnO film. The top view in Fig. 6(a) reveals the uniformity and compactness of the grains. The cross-sectional view in Fig. 6(b) indicates that Li-ZnO columnar grains are clear and at a slight angle from the normal to the substrate, indicating that Li-ZnO grains exhibit good orientation. The piezoelectric effect is such that, when AC voltage is applied to the input IDT and the signal voltage variations were subsequently converted into a mechanical acoustic wave, the other IDT acted as an output receiver that converted mechanical wave vibrations back into an output voltage. The output voltage, or the wave velocity, changed with the thickness of the silicon substrate.

Figure 7 schematically depicts the configuration of the IDT, where λ is the periodicity of the IDT (wavelength of the acoustic wave); L is the length of the IDT fingers; W is the acoustic aperture (length of overlap of the IDT fingers), and d is the length of the path of acoustic propagation. In the design of an IDT, numerous parameters have to be specified. The spacing and electrode width determine the frequency response of the transducer. In the design presented, a split-electrode IDT was adopted, because the problem that results from finger reflections can be greatly diminished using a $\lambda/8$ finger width rather than a $\lambda/4$ finger width, such that the acoustic wave reflections from each split-electrode pair cancel out at the central frequency, rather than adding as in the case of the single-electrode IDT.⁽¹³⁾ Table 2 presents the parameters of the IDT design used herein.

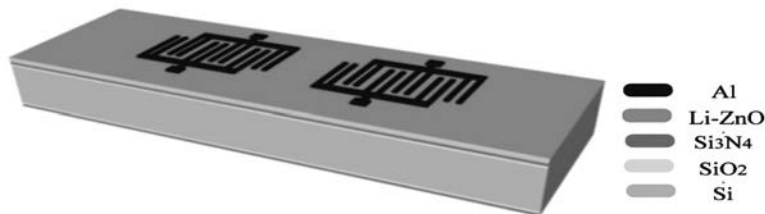


Fig. 4. Schematic diagram of plate wave sensor.

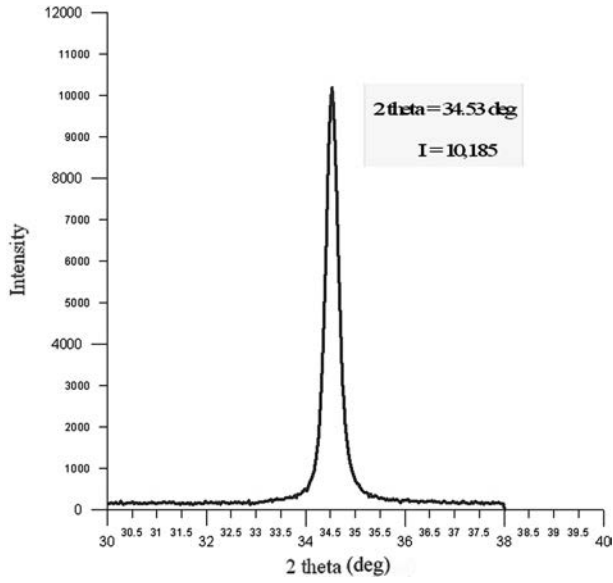


Fig. 5. X-ray diffraction scans of Li-ZnO film.

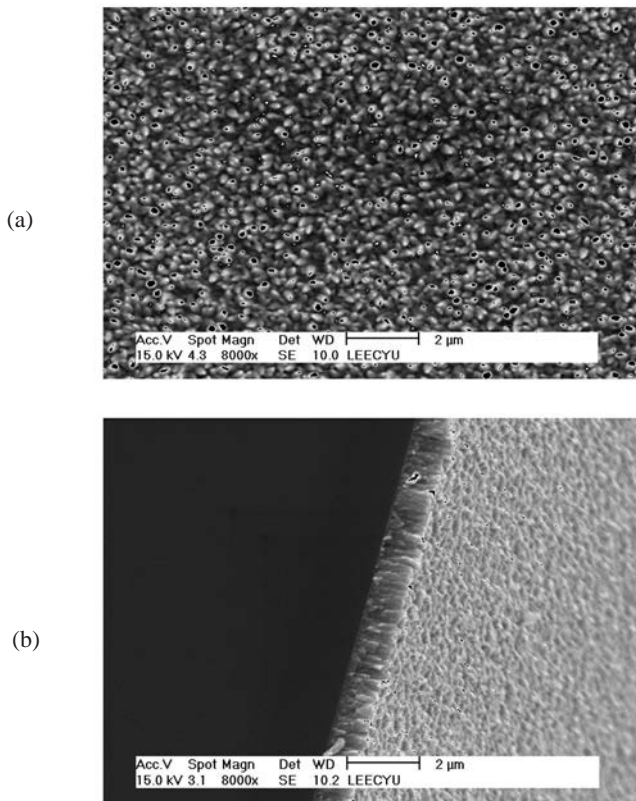


Fig. 6. SEM micrographs of Li-ZnO films: (a) top view and (b) cross-sectional view.

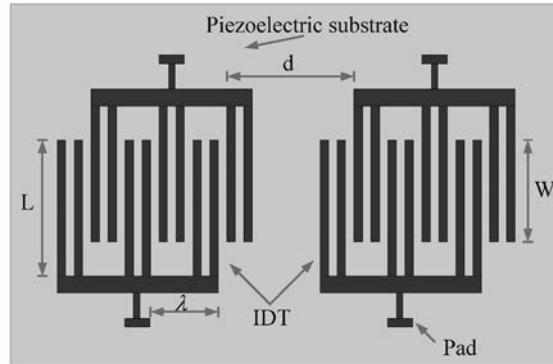


Fig. 7. Sketch of configuration of IDT.

Table 2
IDT design parameters.

Periodicity of IDT (λ)	40 μm
Length of the IDT fingers (L)	2400 μm
Length of overlap of the IDT fingers (W)	2000 μm
Length of the path of acoustic propagation (d)	800 μm
Numbers of pairs (N)	100
Area of pad	600 \times 600 μm^2

3. Device Fabrication

This plate wave sensor was fabricated by the process depicted in Fig. 8. The process was begun with a 308.40- μm -thick, 100-mm-diameter double polished (100) silicon wafer. First, a silicon dioxide (SiO_2) film approximately 1000 \AA thick was dry oxidized before a low-pressure chemical-vapor deposition (LPCVD) silicon nitride (Si_3N_4) film with a thickness of 1500 \AA was deposited to reduce the stress, as depicted in Fig. 8(a). The LPCVD Si_3N_4 film was used as an etching mask at the back of the wafer during wet etching in KOH solution. Then, on the rear side of the silicon substrate, a Shipley S1813 photoresist was coated using a spinner that rotated at a rate of 1000 rpm for 5 s, and then at 4000 rpm for 30 s. The coated substrate was then softbaked at 90°C for 90 s. The etching-hole area pattern was exposed on the photoresist-coated substrate surface using ultraviolet light. Reactive ion etching (RIE) was applied to open the rear side of the etching-hole, as depicted in Fig. 8(b). A Li-ZnO film 1.56 μm thick was sputtered from an RF magnetron sputter, as shown in Fig. 8(c); the sputtering conditions are described in Table 3. IDTs were patterned using semiconductor photolithographic techniques, by which Al was

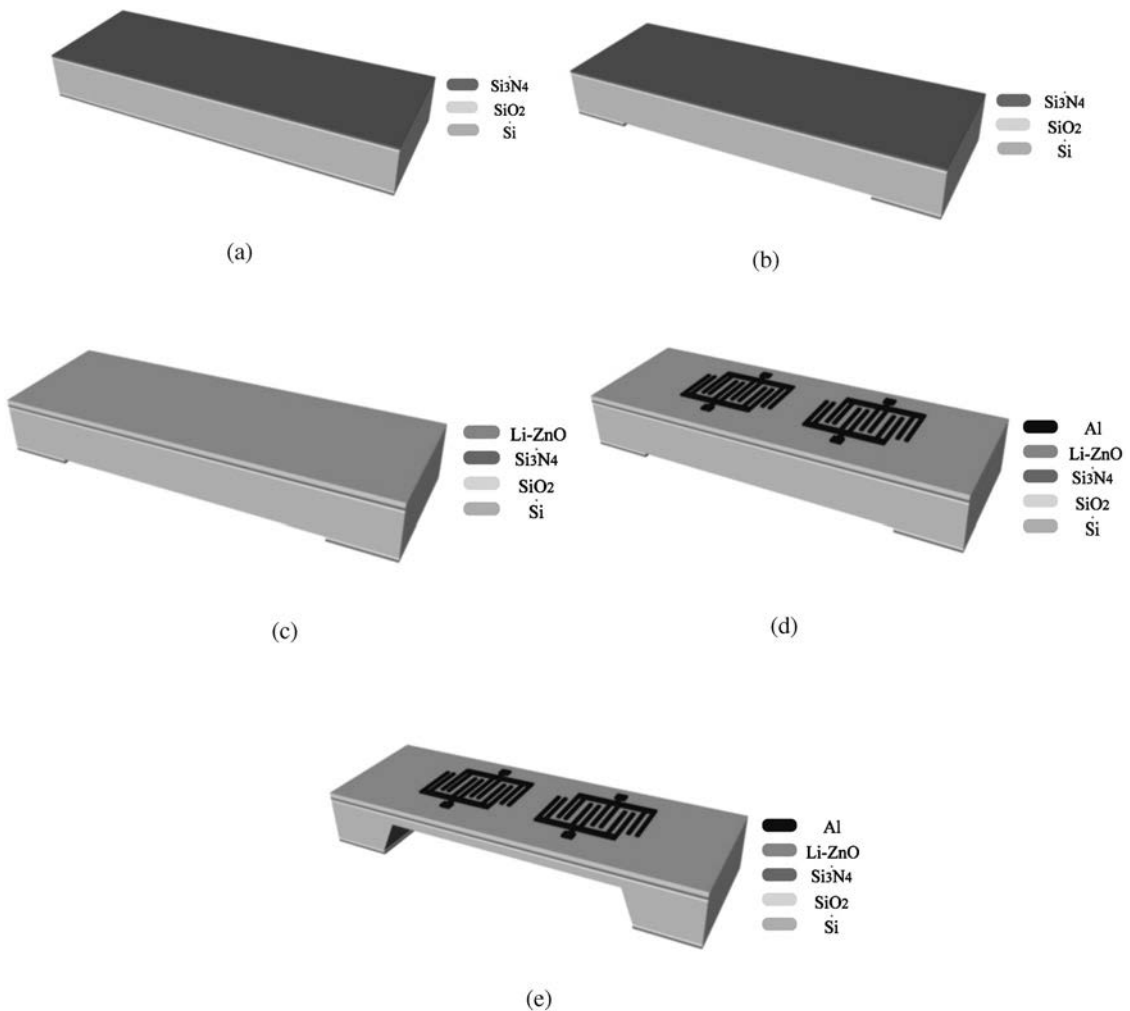


Fig. 8. Process flow of plate wave sensor: (a) growing silicon dioxide film and LPCVD silicon nitride film, (b) defining pattern on rear side of etching-hole, (c) sputtering piezoelectric Li-ZnO film, (d) evaporating Al film and defining pattern of IDTs at 45°, and (e) KOH etching to form silicon membrane.

deposited to a thickness of 1000 Å by E-gun evaporation, as indicated in Fig. 8(d). Finally, a silicon membrane was generated by soaking the rear side of the substrate with 33% in KOH solution at 72°C; the etching rate was 0.94 μm per minute, as shown in Fig. 8(e).

4. Results

The experimental setup for measuring the frequency response and the insertion loss of a plate wave sensor, as illustrated in Fig. 9, includes an HP8714ES network analyzer and an etching holder. An HP8714ES network analyzer monitors with the frequency resolution of

Table 3
Sputtering conditions.

Target	Li-doped ZnO, 4" diameter
Gas (sccm)	Ar/O ₂ = 1 : 1
Deposition pressure (Pa)	4.9×10^{-5}
RF power (W)	200
Substrate temperature (°C)	215
Sputtering rate (Å/h)	3467
Working distance (cm)	13
Postannealing condition	400°C for 1.5 h in air

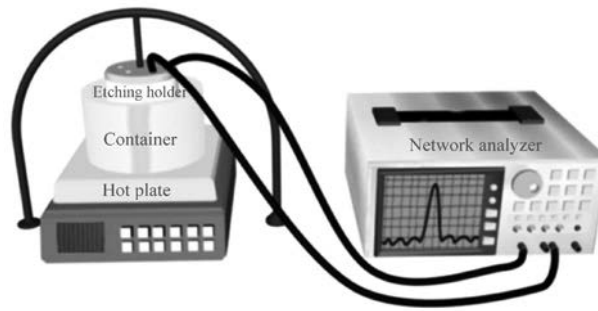


Fig. 9. Experimental setup of plate wave sensor.

0.01 MHz was used to monitor in real-time the thickness of a silicon membrane as the target central frequency was shifted. The measurement accuracy of the central frequency was 0.01 MHz; the accuracy of thickness of silicon membrane was 0.05 μm . The etching process automatically monitors the thickness of a silicon membrane as the frequency changes. First, an Alpha-step 500 surface profiler was used to measure the initial total thickness of 308.40 μm thick silicon. The central frequency of the experimental unetched wafer was 112.40 MHz. Then, the first etching of silicon was measured as 145.90 μm thick. The experimental result for the first etching central frequency was also 112.40 MHz. Now, the thickness of a silicon membrane could then be determined, and it was 162.50 μm . Repeating these steps reveals that, the second etching of silicon was measured at 282.30 μm thick, and experimental result for the second etching central frequency was 108.70 MHz; the thickness of the silicon membrane was 26.10 μm ; the experimental results are described in Table 4. Figure 10 compares the simulation and experimental results of silicon thickness with respect to frequency. Figure 10 reveals that the error between the simulation and the experimental results is less than 1.50 μm , implying close correspondence.

Table 4
Experimental results.

	Etch depth of silicon (μm)	Thickness of silicon (μm)	Central frequency (MHz)	Amount of shift the central frequency (MHz)	Insertion loss S_{21} (dB)
Unetch silicon	0	308.40	112.40	0	-38.60
First etching of silicon	145.90	162.50	112.40	0	-38.60
Second etching of silicon	282.30	26.10	108.70	3.7	-57.50

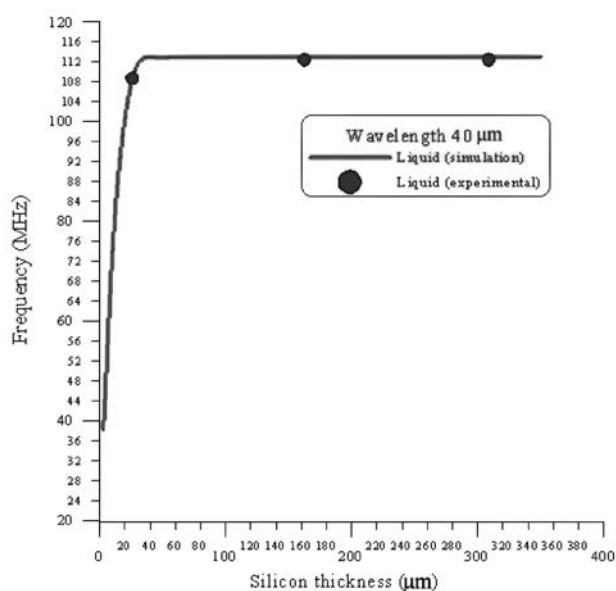


Fig. 10. Comparison of simulation and experimental results of thickness of silicon with respect to frequency.

5. Conclusions

This work presents a plate wave sensor for monitoring the thickness of a silicon membrane from 20 μm to 40 μm in real-time during wet etching. The proposed plate wave sensor allows the thickness of a silicon membrane, from a few μm to hundreds of μm , to be monitored, depending on the periodicity of the IDT. Therefore, an IDT with the proper periodicity is suitable for monitoring the thickness of a silicon membrane. The theoretical

and measured values differ by an error of less than 1.50 μm , so the experimental and theoretical values correlate well with each other.

Acknowledgements

This work was accomplished with much needed support and the authors would like to thank the National Science Council of R. O. C. through grant NSC 94-2218-E-155-001 for financial support. The authors also thank Kai-Hsiang Yen, Fu-Yuan Xiao, Ying-Chou Cheng, Shih-Yung Pao, Wen-Jong Chen and Chia-Hua Chu of the Institute of Applied Mechanics, National Taiwan University, and professors Tsung-Tsong Wu, Lung-Jieh Yang and Chien-Liu Chang for their valuable advice and assistance in performing the experiments. In addition, we would finally like to thank the NSC Northern Region MEMS Research Center for kindly making their complete research facilities available.

References

- 1 K. Minami, H. Tosaka and M. Esashi: *J. Micromech. Microeng.* **5** (1995) 41.
- 2 M. Madou: *Fundamentals of Microfabrication* (CRC Press, New York, 1997) p. 193.
- 3 C. M. A. Ashruf, P. J. French, P. M. Sarro, P. M. M. C. Bressers and J. J. Kelly: *Mechatronics* **8** (1998) 595.
- 4 P. Z. Chang and L. J. Yang: *J. Micromech. Microeng.* **8** (1998) 182.
- 5 C. Y. Lee, Y. C. Cheng, T. T. Wu, Y. Y. Chen, W. J. Chen, S. Y. Pao, P. Z. Chang, P. H. Chen, K. H. Yen and F. Y. Xiao: *Tamkang Journal of Science and Engineering* **7** (2004) 61.
- 6 C. Y. Lee, Y. C. Cheng, Y. Y. Chen, P. Z. Chang, T. T. Wu, P. H. Chen, W. J. Chen and S. Y. Pao: *Jpn. J. Appl. Phys.* **43** (2004) 3611.
- 7 T. T. Wu and M. P. Chang: *Jpn. J. Appl. Phys.* **41** (2002) 5451.
- 8 T. T. Wu and T. Y. Wu: *Trans. ASME* **66** (2002) 262.
- 9 M. B. Braga: *Wave Propagation in Anisotropic Layered Composites*, Ph.D. dissertation, Stanford University, Stanford, CA, 1990.
- 10 B. A. Auld: *Acoustic Fields and Waves in Solid* (R. E. Krieger, New York, 1990) Vol. 1 p. 359.
- 11 K. Uchino: *Ferroelectric Devices* (Marcel Dekker, New York, 2000) p.67.
- 12 T. Mitsuyu, S. Ono and K. Wasa: *Jpn. J. Appl. Phys.* **51** (1980) 2464.
- 13 C. K. Campbell: *Surface Acoustic Wave Devices for Mobile and Wireless Communication* (Academic Press, New York, 1998) p. 183.